MR Evaluation of Hydrocephalus

Taher El Gammal, Marshall B. Allen, Jr., Betty Sue Brooks and Edward K. Mark

AJNR Am J Neuroradiol 1987, 8 (4) 591-597
http://www.ajnr.org/content/8/4/591

MR Evaluation of Hydrocephalus

Taher El Gammal[1]
Marshall B. Allen, Jr.[2]
Betty Sue Brooks[1]
Edward K. Mark[2]

An analysis of sagittal T1-weighted MR studies was performed in 23 patients with hydrocephalus, 58 patients with atrophy, and 100 normal patients. The average mamillopontine distance was 1.15 cm for the normal group, 1.2 cm for patients with atrophy, and 7.5 mm for patients with hydrocephalus. A reduction of the mamillopontine distance below 1.0 cm was found in 22 patients with hydrocephalus, 5 patients with atrophy, and 15 normal patients. Dilatation of the anterior third ventricle was noted in 21 patients in the hydrocephalus group and in none of the patients in the atrophy and normal groups. The average thickness of the corpus callosum at the level of the foramen of Monro was 6 mm in normal subjects and was reduced below 6 mm in 16 of the hydrocephalus patients. Smooth elevation of the corpus callosum was noted in 20 hydrocephalus patients, in 2 patients with atrophy, and in none of the normal patients. MR improves the accuracy of diagnosis in patients with hydrocephalus both because of its ability to show small obstructing lesions that are not depicted by CT and because the mass effect of the distended supratentorial ventricles produces anatomic changes that are delineated with precision by MR.

CT provides incomplete information for diagnosing hydrocephalus produced by very small or isodense pathologic changes in the aqueduct and in the foramen of Monro [1, 2]. Even with advanced CT techniques, use of contrast media in the subarachnoid space and ventricular system was essential in the CT evaluation of some cases of hydrocephalus [3–5].

MR with a high-field-strength magnet has returned to neuroimaging the more detailed anatomic studies of the midline ventricles and surrounding brain tissue in the lateral view that used to be achieved with high-quality pneumoencephalography. This is achieved noninvasively and without alteration of the CSF dynamics.

MR is superior to CT in the diagnosis of hydrocephalus because of its ability to visualize small obstructing lesions in relation to the midline structures, which CT is unable to depict (Figs. 1–4). The enhanced CT in all the cases illustrated only showed dilatation of the lateral ventricles. MR studies, however, showed the site and the nature of the obstructing lesions.

MR also clearly outlined the anatomic changes caused by distention of the lateral and third ventricles from obstruction of CSF pathways. This report focuses on the changes of the distended supratentorial ventricles in hydrocephalus as seen by MR and compares them with normal studies and with cases showing evidence of atrophy.

Materials and Methods

Sixty-six patients with varying degrees of hydrocephalus were examined by MR during a period of 9 months. Of these, the MR findings of 23 patients with moderate or severe hydrocephalus with distention of the lateral and third ventricles were selected for study. These studies were compared with MR examinations of 58 patients whose MR studies were thought to be consistent with varying degrees of cerebral atrophy. Twenty-five patients were

This article appears in the July/August 1987 issue of *AJNR* and the October 1987 issue of *AJR*.

Received March 31, 1986; accepted after revision January 2, 1987.

Presented in part at the 24th annual meeting of the American Society of Neuroradiology, San Diego, January 1986.

[1] Department of Radiology, Section of Neuroradiology, Medical College of Georgia, 1120 15th Street, Augusta, GA 30912. Address reprint requests to T. El Gammal.

[2] Department of Surgery, Section of Neurosurgery, Medical College of Georgia, Augusta, GA 30912.

***AJNR* 8:591–597, July/August 1987**
0195–6108/87/0804–0591

classified as having mild atrophy and 33 as having moderate atrophy. One hundred patients whose MR studies were evaluated as normal were also included in the analysis.

The hydrocephalus patients ranged in age from 2 months to 68 years, with five patients under age 20. There were 16 females and 7 males. One patient had postinflammatory obstruction at the foramen of Monro with intraventricular bands, eight patients had aqueduct obstruction (three were due to nontumorous stenosis, two to gliomas, two to pinealomas, and one to thalamic abscess extending into the mesencephalon). There were eight posterior fossa tumors (five acoustic neurinomas, one Chiari I malformation, one choroid plexus papilloma, and one medulloblastoma). Six cases of extraventricular obstructive hydrocephalus were also included, of whom only one had known definite etiology of the obstruction (subarachnoid hemorrhage).

Fifty-eight consecutive patients with atrophy, including 26 men and 32 women ranging in age from 27 to 85 years, were also studied.

One hundred consecutive normal MR studies were obtained from volunteers, patients with psychosomatic complaints, and patients with clinical symptoms of neurologic disease such as headaches and seizures. There were 63 women and 37 men, ranging in age from 21 to 78 years.

The MR examinations were obtained on a 1.5-T superconductive magnet. Sagittal images were obtained using 3-mm-thick sections spaced 0.6 mm apart, with four excitations, an echo delay time (TE) of 25 msec, and a repetition time (TR) of 800 msec. The field of view was 24 cm.

Measurements were obtained on the radiograph hard copies (15 images exposed on a 14 × 17 radiograph). The 24-cm field of view was used for all cases, and the measurements were converted to life-size by computer analysis. The following observations and measurements were made in all cases from the lateral T1-weighted images: (1) Appearance of the anterior third ventricle; (2) Mamillopontine distance; (3) Distance between corpus callosum and posterior fornix; (4) Corpus callosum shape and thickness measured at the level of the foramen of Monro; and (5) CSF flow-void signal in the aqueduct and the third ventricle.

Results

Distension of the lateral and third ventricles due to CSF obstruction produces anatomic changes that are clearly delineated on high-resolution T1-weighted lateral MR images (see Table 1). The measurements and appearance of the normal anatomy in relation to the third ventricle and corpus callosum are distinctly different from the appearance when there is cerebral atrophy or significant obstruction of the CSF pathways.

Anterior Third Ventricle

In all normal studies and in cases with atrophy, the anterior third ventricle appeared collapsed with small anterior recesses. In the hydrocephalus group, 21 of 23 cases showed

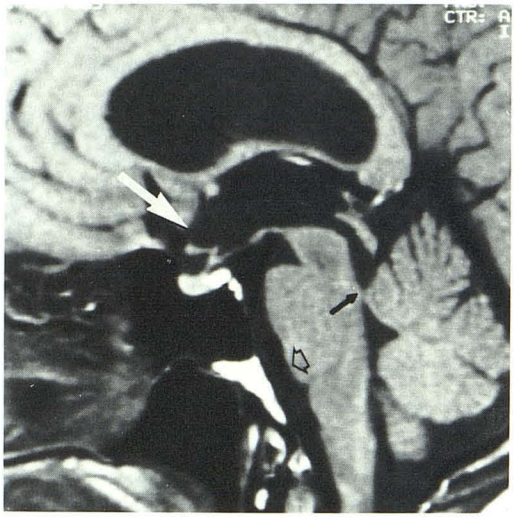

Fig. 2.—Aqueduct stenosis in a 45-year-old man. This was diagnosed only on MR. Enhanced CT scan, not shown, demonstrated dilated lateral ventricles. Lateral T1-weighted image (TR = 800, TE = 25 msec) shows focal stenosis of aqueduct (*black arrow*). Note also the lobulation of pons (*open arrowhead*) and dilated anterior third ventricle (*white arrow*). Mamillopontine distance is reduced.

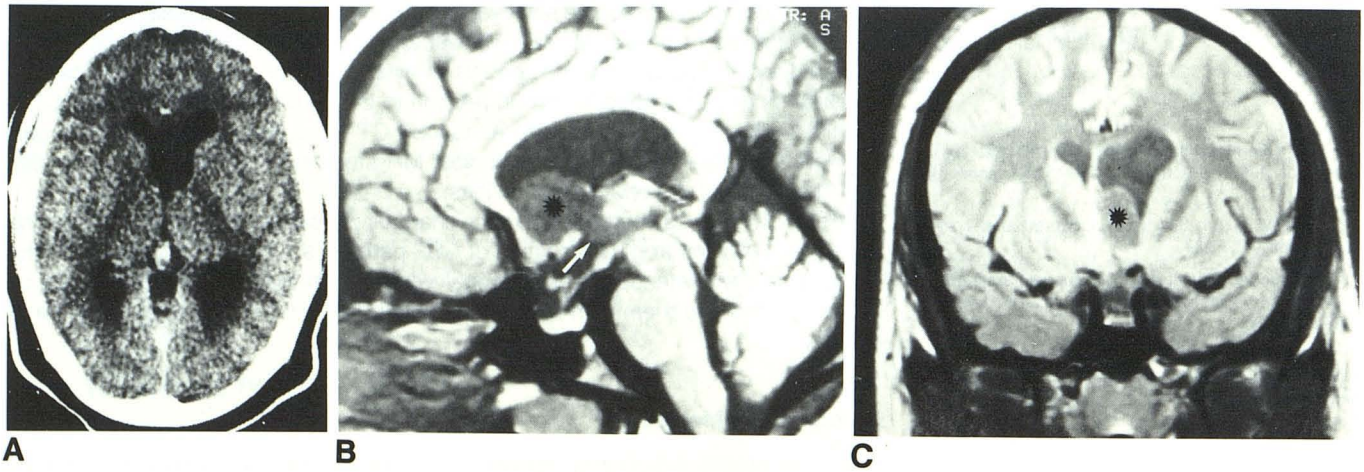

Fig. 1.—Hypodense nonenhancing colloid cyst not diagnosed by CT.
***A*, Transaxial enhanced CT shows unilateral dilatation of left lateral ventricle. The cause is not apparent.**
***B*, Sagittal T1-weighted MR reveals colloid cyst at foramen of Monro extending into third ventricle (*arrow*) and left lateral ventricle (*asterisk*). Optic recess of third ventricle is dilated. (TR = 800, TE = 25 msec)**
***C*, Coronal section shows colloid cyst (*asterisk*) in left lateral ventricle. (TR = 2000, TE = 25 msec)**

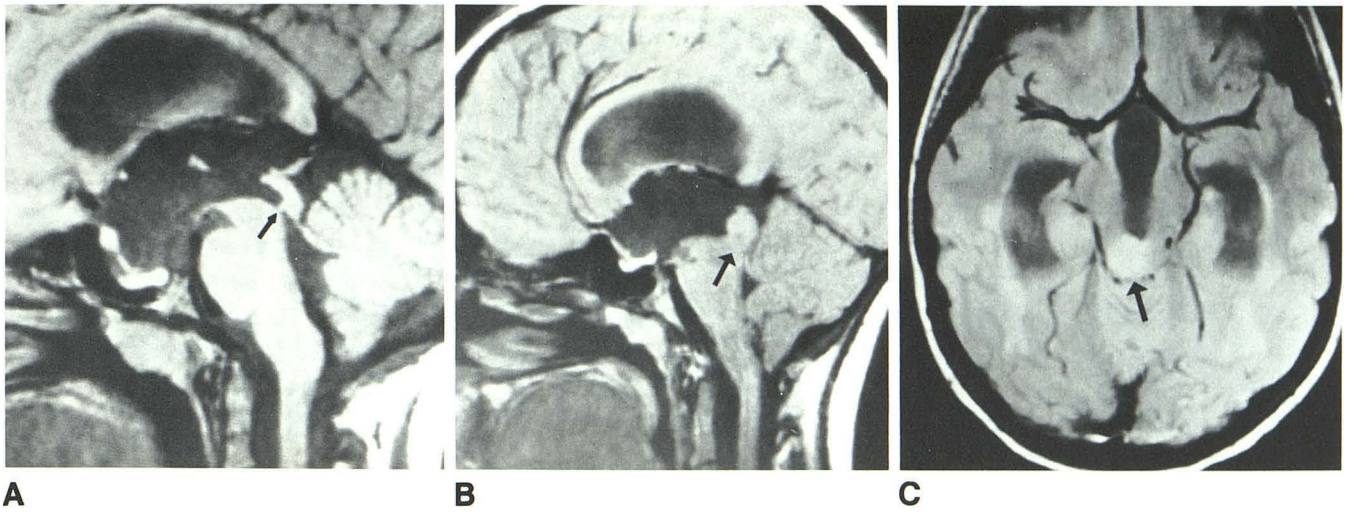

Fig. 3.—Aqueduct obstruction not shown by enhanced CT.

***A*, Nonneoplastic aqueduct stenosis (*arrow*). Note normal quadrigeminal plate (TR = 800, TE = 25 msec). There is significant forward displacement of optic chiasm and pituitary infundibulum by massively dilated anterior third ventricle.**

***B* and *C*, Small right quadrigeminal plate tumor producing aqueduct obstruction. In *B*, note rounded slight enlargement of quadrigeminal plate in relation to aqueduct obstruction (*arrow*). Patient has massive dilatation of third ventricle with significant elevation and thinning of corpus callosum and reduced mamillopontine distance. Transaxial view in *C* shows high signal (*arrow*) in right side of quadrigeminal plate. (TR = 2000, TE = 25 msec)**

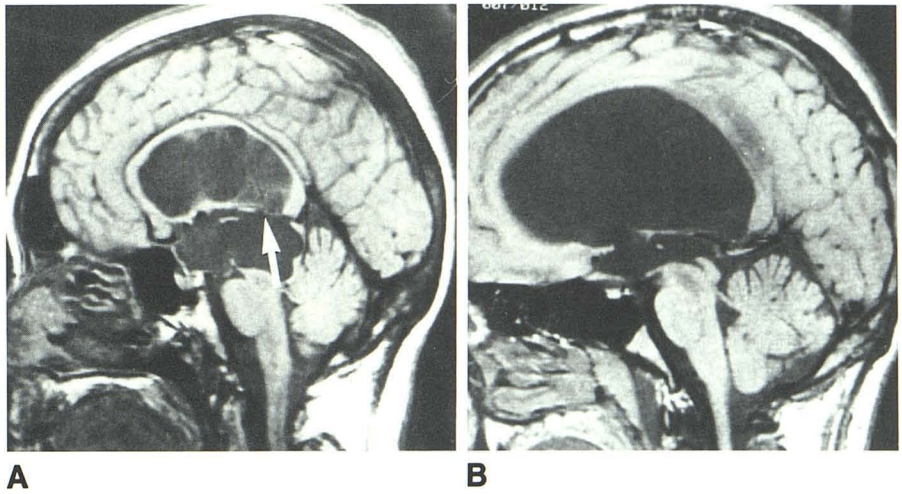

Fig. 4.—Effects of dilated third ventricle in two cases of benign aqueduct stenosis.

***A*, Massive dilatation of third ventricle. Posterior third ventricle is also massively dilated, preventing downward displacement of posterior fornix (*arrow*). Dilated upper aqueduct is assimilated into cavity of third ventricle. Note very thin rim of quadrigeminal plate between dilated posterior third ventricle and precentral cerebellar vein. Mamillary body almost touches top of pons.**

***B*, Another patient with aqueduct stenosis. Quadrigeminal plate appears normal. Posterior third ventricle is not dilated, allowing downward displacement of posterior fornix. Anterior third ventricle is also dilated with reduction of mamillopontine distance.**

variable distention of the anterior third ventricle; massive dilatation and ballooning was noted in nine of these.

Appearance and Thickness of Corpus Callosum

The average thickness of the corpus callosum in normal studies was measured as 2.2 mm on the radiograph (6 mm actual patient measurement). Depressions and defects on its superior surface were found in 36% of the cases. In 13% the corpus callosum was relatively thick. The inferior margin appeared regular and smooth.

With hydrocephalus, 20 of 23 patients showed a rounded elevation of the corpus callosum with uniform smooth thinning. In the atrophy group, the thickness of the corpus callosum was reduced, and the reduction paralleled the severity of the atrophy. In 25 patients with mild atrophy, only two had thicknesses that measured less than 2 mm (6 mm), while 19 of 33 patients having moderate atrophy showed a measurement less than 2 mm (6 mm). In five of the latter cases, the thinning of the corpus callosum was very irregular (Fig. 5A).

MP Distance (Fig. 6)

In normal patients, the average measurement was 3.8 mm on radiographs (1.15 cm actual patient measurement) with a standard deviation of 0.3 mm (0.9 mm). A reduced mamillopontine distance below 3.5 mm (1 cm) was noted in 22 of 23 patients with hydrocephalus. In some patients the mamillary body touched the pons. Reduction of the mamillopontine distance in four patients was thought to be due partly to the

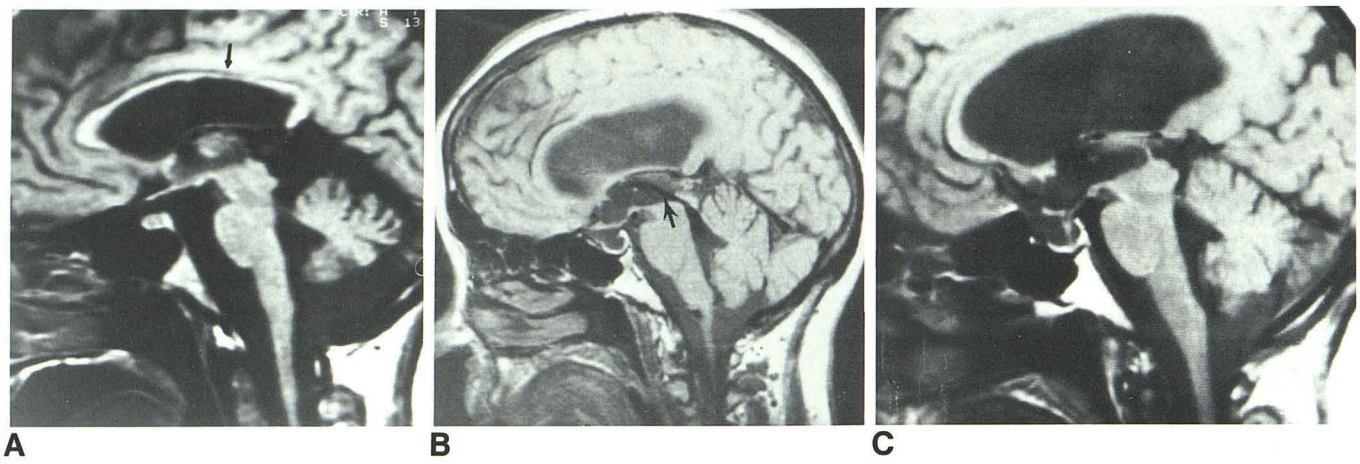

Fig. 5.—Comparison between atrophy and hydrocephalus.

***A*, Patient with atrophy. There is irregular thinning of corpus callosum, which remains flat without elevation (*arrow*). Also note normal mamillopontine distance and appearance of anterior third ventricle.**

***B* and *C*, Extraventricular obstructive hydrocephalus. Patient had positive isotope cisternography with persistent uptake in lateral ventricles up to 48 hr. Clinical features were consistent with "normal pressure" hydrocephalus. There is dilatation of optic recess of third ventricle (*C*). Patient also had empty sella, possibly due to intermittent increased CSF pressure. Flow-void signal in third ventricle, possibly due to reflux, is noted in *B* (*arrow*). Note thinning and elevation of corpus callosum, depression of posterior fornix, and reduction of mamillopontine distance. (TR = 800, TE = 25 msec)**

TABLE 1: MR Observations and Measurements in 100 Normal Patients and in Patients with Hydrocephalus (23) and Atrophy (58)

Findings	Normal Patients	Hydrocephalus	Atrophy
Dilated anterior third ventricle	0	21 (9, massive dilatation)	0
Average MP distance	3.8 mm (1.15 cm)*	2.5 mm (7.5 mm)*	4.0 (1.2 cm)*
Diminished MP distance 3.5 mm (1 cm) and below	15 (2, advanced empty sella; 7, angle between medulla and spinal cord)	22 (a few, mamillary body touched pons; 4, reduction was partly due to posterior fossa tumor)	5
Corpus-fornix distance	Range, 0–3 mm (0–8 mm)*; 2, more than 2 mm (6 mm)*	Range, 4–10 mm (1.2–3 cm)*; 15, more than 5 mm (1.5 cm)*	Range, 0–5 mm (0–1.5 cm)*; 30, more than 2.5 mm (7.5 mm)*
Corpus callosum thickness	6, below 2 mm (6 mm)*; range, 1.7–3 mm (5–9 mm)*; average, 2.2 mm (6 mm)*; 13, 2.5–3 mm (7.5–9 mm)*	16, below 2 mm (6 mm)*; range, 0.5–2 mm (1.5–6 mm)*	21, below 2 mm (6 mm)*; range, 1–3 mm (3–9 mm)*
Corpus callosum shape	No elevation in 100; 36, depressions and defects, mostly posterior	20, smooth round elevation; 2, irregular thin corpus	2, elevated corpus, mild in 1; 5, irregular corpus callosum
Void signal	19	14	24
Aqueduct only	17	1	17
Also in third ventricle (possible reflux)	2	13	7

Note.—MP = mamillopontine.

* Radiograph measurement and corrected actual patient measurement (in brackets).

elevated pons consequent to a posterior fossa mass.

In the atrophy group, the average mamillopontine distance was slightly higher than normal, 4 mm on radiographs (1.2 cm actual patient measurement). In 15% of normal patients, the mamillopontine distance was below 1 cm (actual patient measurement). In 50% of these cases there was angulation between the medulla oblongata and the spinal cord. In the normal group, such angulation was found in only 14 (14%) of the studies. And in seven (50%) of these, the mamillopontine distance was below 1 cm (actual measurement).

Distance Between Corpus Callosum and Posterior Fornix

With hydrocephalus, the distended lateral ventricles tend to depress the posterior fornix. In 98% of the normal group, the corpus callosum posterior fornix distance was less than

Fig. 6.—Measurement of mamillopontine distance made on normal, lateral T1-weighted image. Distance is measured from anterior base of mamillary body to top of pons parallel to anterior aspect of mesencephalon. Note normal thickness and shape of corpus callosum, and normal appearance of anterior inferior third ventricle. (TR = 800, TE = 25 msec)

2 mm on radiographs (6 mm actual patient measurement). Fifteen of 23 hydrocephalus cases had measurements of more than 3 mm (9 mm).

CSF Flow-Void Signal

In 19% of the normal group, there was evidence of a void signal in the aqueduct. In only 2% there was also linear void signal in the cavity of the third ventricle, which may suggest reflux movement of CSF from the aqueduct into the third ventricle. In the hydrocephalus group, 14 of 23 patients had void signal in the aqueduct. All except one also showed a linear void signal in the third ventricle, suggesting reflux (Figs. 5B and 7). Four of the 23 patients had obstruction or obliteration of the aqueduct with no void signal. Therefore, in 14 of 19 patients with hydrocephalus in whom the aqueduct was patent, a CSF flow-void signal was observed. In the atrophy group, 24 of 58 patients had a void signal. Seven of these also showed linear void signal in the third ventricle.

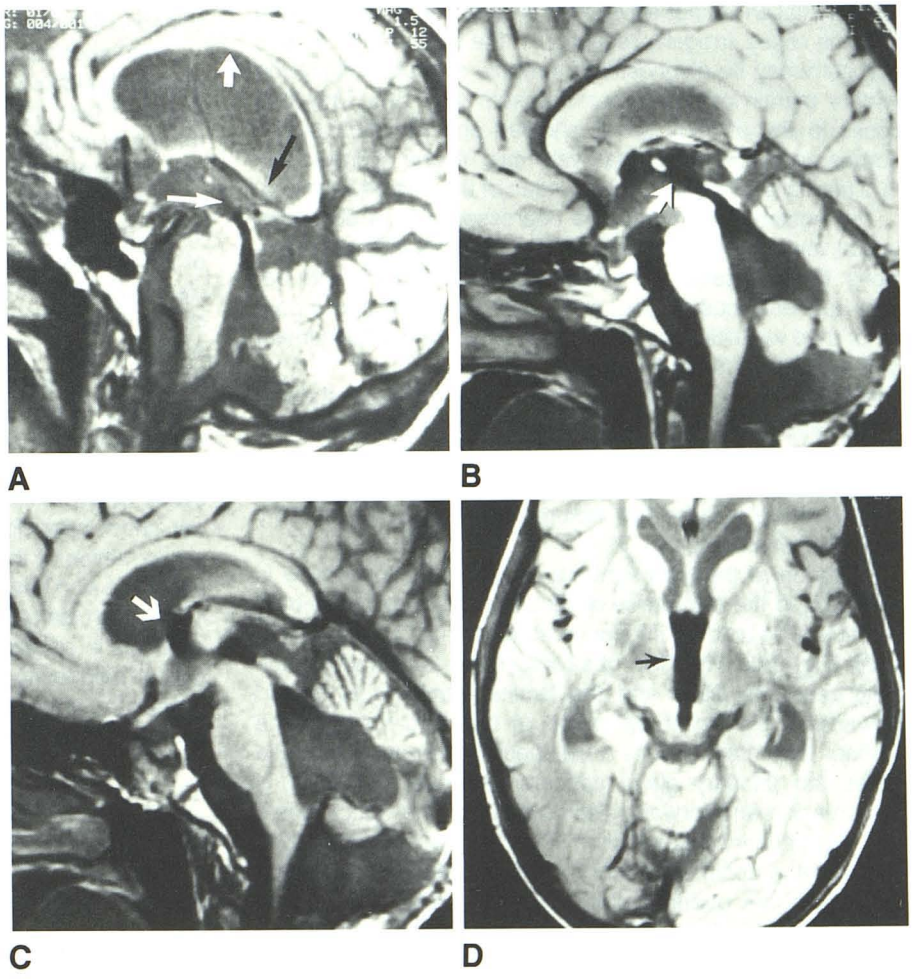

Fig. 7.—Void signal due to CSF movement in third ventricle.

***A*, 56-year-old woman with extraventricular obstructive hydrocephalus of unknown origin. Corpus callosum is elevated with uniform thinning (*thick white arrow*) and posterior fornix is depressed (*black arrow*). Note low signal in aqueduct and third ventricle due to CSF movement (*thin white arrow*).**

***B*, 7-year-old girl with medulloblastoma and extraventricular obstructive hydrocephalus. Midsagittal section shows CSF movement (*arrow*) into third ventricle. (TR = 800, TE = 25 msec)**

***C*, Adjacent parasagittal image shows advancement of low signal to foramen of Monro (*arrow*).**

***D*, Transaxial image shows low signal within third ventricle (*arrow*). (TR = 2000, TE = 25 msec)**

Discussion

MR demonstrates with precision and detail the cause and site of obstruction in many patients with hydrocephalus; and the outline of the cerebral structures particularly in the midline by MR is far superior to that of CT (Figs. 1–4, 5B, and 5C).

Hydrocephalus produces increased intraventricular pressure with the result that the dilated supratentorial ventricles act like a mass to produce compression and displacement of adjacent brain structures. The following MR findings are suggestive of CSF pathways obstruction:

1. Dilatation of the anterior third ventricle.
2. Inferior bowing and displacement of the hypothalamus with reduction in the mamillopontine distance.
3. Depression of the posterior fornix with increase in the superior inferior dimensions of the lateral ventricles.
4. Uniform smooth thinning and elevation of the corpus callosum.
5. Intraventricular flow void due to CSF movement.
6. Paraventricular high signal on proton density and on T2-weighted images.

Stretching and upward displacement, as well as smooth and relatively uniform thinning of the corpus callosum, occurs in patients with hydrocephalus consequent to the lateral ventricle distention (Figs. 2–4, 5B, and 7A). In patients with atrophy, although there is thinning of the corpus callosum, it appears flat and is not elevated in the majority of cases. Also, in some cases, irregular reduction in the mass of the corpus callosum may be diagnostic of atrophy, especially along the inferior margin of the corpus callosum (Fig. 5A). Only two cases in the atrophy group showed any elevation of the corpus callosum, which was very mild in one. None of the 100 normal studies showed elevation of the corpus callosum.

The posterior fornix may be depressed due to distended lateral ventricles with increase in their superior inferior dimensions. In some cases of hydrocephalus, particularly with benign aqueduct obstruction, excessive distention of the posterior third ventricle may prevent the downward displacement of the posterior fornix (Fig. 4B).

All patients in the normal and atrophy groups showed normal appearance of the anterior inferior third ventricle, and 21 of the 23 cases of advanced hydrocephalus had dilatation of the anterior third ventricle. The appearance of the anterior third ventricle is a helpful feature in distinguishing atrophy from CSF obstruction [6, 7].

Dilatation of the third ventricle in patients with atrophy is seen only in the transverse diameter of the body of the third ventricle. The anterior inferior recesses remain collapsed and small (Fig. 5A). With CSF obstruction, the optic and infundibular recesses dilate and the lamina terminalis is bowed forward. In significant distention of the third ventricle the anterior third may assume a ballooned appearance. In these cases the pituitary gland appears flattened and there is compression and forward displacement of the optic chiasm and the pituitary infundibulum (Fig. 3). The posterior third ventricle and upper aqueduct may also dilate with significant atrophy of the quadrigeminal plate (Fig. 4A). The general distention of the third ventricle will also result in downward displacement of the hypothalamus with reduction of the mamillopontine distance.

The mamillopontine distance (Fig. 6) is measured from the anterior root of the mamillary body to the top of the pons parallel to the anterior mesencephalon. The normal average distance was found to be 3.8 mm on the radiograph, which is about 1.15 cm calculated actual life-size. In 85% the actual measurement was 1 cm or more. In patients with advanced hydrocephalus, the mamillopontine distance was diminished in virtually every case. In the atrophy group the average mamillopontine distance was 4.0 mm (true measurement of 1.2 cm).

Increased intraventricular pressure and ventricular distention may result in rupture of the ventricular ependyma and increased transependymal transport of CSF, with resultant increase in water content in the periventricular region resulting in high signal on T2-weighted sequences. Periventricular high signal surrounding the third and fourth ventricles and temporal horns may also be observed in some cases of hydrocephalus. A thin crescent of high signal, especially in relation to the angles of the frontal horns, is a normal finding on T2-weighted images. This has been recently observed in over two-thirds of normal MR examinations [8]. Since periventricular high signal on T2-weighted images is commonly observed in middle-aged and elderly patients, the value of this sign as a differentiating feature between hydrocephalus and atrophy is limited in these age groups.

Direct observation of CSF movement can be made on MR examination from the appearance of a void within the aqueduct and third ventricle and in a few patients at the level of the foramen of Monro [9, 10]. CSF flow normally has a pulsatile and bidirectional component [11]. The void signal is more frequently seen in patients with hydrocephalus, however, and we believe that this is due to an increased incidence of CSF movement and possible reflux as shown by isotope cisternography. The linear appearance of the flow-void signal in the third ventricle suggests a reflux of the CSF from the aqueduct (Figs. 5B and 7). The void signal was noted in 19% of the normal group, in 41% of the atrophy group, and in 74% of hydrocephalus cases without distortion or obstruction of the aqueduct. Only two of the normal patients also had a void signal, with possible reflux, in the third ventricle. In the 14 cases of hydrocephalus with flow-void signal, only one did not show void signal in the third ventricle. In the atrophy group, seven of the 17 cases that showed void signal in the aqueduct also had flow-void signal in the third ventricle.

Although the differential diagnosis of atrophy versus hydrocephalus in elderly patients with dilated ventricles remains a difficult diagnostic problem, because CSF obstruction may be associated with brain atrophy, MR can still provide helpful ancillary information in some cases.

Summary

In the evaluation of patients with hydrocephalus, MR illustrates the anatomic changes that occur with increased intraventricular pressure and ventricular distention better than CT

does, in part because of its multiplanar imaging capability and particularly because of the value of its lateral projection. Differentiation between patients with extraventricular obstructive hydrocephalus and cerebral atrophy is improved with MR, and MR may demonstrate a cause of obstruction that is not adequately outlined by CT, either because of the small size of the obstruction, lesion location, or attenuation. Preliminary MR observations related to dynamics of the CSF flow indicate that MR also has great potential for contributing to a better understanding of CSF circulation. Further investigation in this area should prove rewarding.

REFERENCES

1. El Gammal T, Allen MB Jr, Lott T. Computer assisted tomography and pneumoencephalography in nontumorous hydrocephalus in infants and children. *J Comput Assist Tomogr* **1977**;1(2):204–210
2. El Gammal T, Brooks BS. Lesions at the foramen of Monro: evaluation by computed tomography, angiography, and pneumoencephalography. *South Med J* **1983**;76(12):1515–1523
3. Madrazo I, Garcia Renteria JA, Paredes G, Olhagaray B. Diagnosis of intraventricular and cisternal cysticercosis by computerized tomography with positive intraventricular contrast medium. *J Neurosurg* **1981**;55:947–951
4. Nakstad P, Sortland O, Hovind K. The evaluation of ventriculography as a supplement to computed tomography. *Neuroradiology* **1982**;23:85–88
5. Brooks BS, El Gammal T. Metrizamide CT ventriculography in the evaluation of a pseudoballooned fourth ventricle. *AJNR* **1984**;5:825–827
6. El Gammal T. Extraventricular (communicating) hydrocephalus: some observations on the midline ventricles. *AJR* **1969**;106:308–328
7. El Gammal T, Allen MB. An atlas of polytomepneumography. Springfield: Charles C. Thomas, **1977**:175–249
8. Zimmerman RD, Fleming CA, Lee B, Saint-Louis LA, Deck M. Periventricular hyperintensity as seen by magnetic resonance: prevalence and significance. *AJNR* **1986**;7:13–23
9. Sherman JL, Citrin CM. Magnetic resonance demonstration of normal CSF flow. *AJNR* **1986**;7:3–6
10. Rubin JB. Part 1. Imaging spinal CSF pulsation by 2DFT magnetic resonance: significance during clinical imaging. Part 2. Harmonic modulation of proton MR precessional phase by pulsatile motion: origin of spinal CSF flow phenomenon. Presented at the 24th annual meeting of the American Society of Neuroradiology. San Diego, CA, January **1986**
11. du Boulay GH. Pulsatile movements in the CSF pathways. *Br J Radiol* **1966**;39:255–262